Quantitative multiplexed proteomics of mouse microglia by flow-cytometric sorting reveals a core set of highly-abundant microglial proteins

Sruti Rayaprolu[1], Tianwen Gao[1,3], Hailian Xiao[1], Supriya Ramesha[1], Duc M. Duong[1,2], Eric B. Dammer[1,2], James J. Lah[1], Allan I. Levey[1], Nicholas T. Seyfried[1,2]*, and Srikant Rangaraju[1]*

[1]Department of Neurology, Emory University, Atlanta, GA 30322, USA
[2]Department of Biochemistry, Emory University, Atlanta, GA 30322, USA
[3]Xiangya Hospital, Central South University, Changsha, Hunan, 410008, China

*Correspondence should be addressed to:

Nicholas Seyfried, PhD and Srikant Rangaraju, MD

Emory University School of Medicine
Whitehead Biomedical Research Building
615 Michael Street
Atlanta, GA 30322
E-mail: nseyfri@emory.edu, srikant.rangaraju@emory.edu
Phone: (404)-712-8589

ABSTRACT

Background

Proteomic characterization of microglia has been limited by low yield and contamination by non-microglial proteins in magnetic-activated cell sorting (MACS) enrichment strategies. To determine whether a fluorescence-activated cell sorting (FACS)-based strategy overcomes these limitations, we compared microglial proteomes of MACS and FACS-isolated $CD11b^+$ microglia in order to identify core sets of microglial proteins in adult mouse brain tissue.

Results

Quantitative multiplexed proteomics by tandem mass tag mass spectrometry (TMT-MS) of MACS-enriched (N = 5) and FACS-isolated (N = 5) adult wild-type $CD11b^+$ microglia identified 1,791 proteins, of which 953 were differentially abundant, indicating significant differences between both approaches. While the FACS-isolated microglia proteome was enriched with cytosolic, endoplasmic reticulum and ribosomal proteins involved in protein metabolism and immune system functions, the MACS-enriched microglia proteome was enriched with proteins related to mitochondrial function and synaptic transmission. As compared to MACS, the FACS microglial proteome showed strong enrichment for canonical microglial proteins while neuron, astrocyte, and oligodendrocyte proteins were depleted. We identified a core set of proteins highly abundant in microglia including Msn and Cotl1 which were validated in immuno-histochemical studies. By comparing FACS-isolated microglia proteomes with transcriptomes, we observed highly concordant as well as highly discordant proteins that were abundant at the protein level but low at the transcript level.

Conclusions

We demonstrate that TMT-MS proteomics of FACS isolated adult mouse microglia is superior to column-based enrichment approaches, resulting in purer and more highly-enriched microglial proteomes. We also define core sets of highly-abundant adult microglial proteins that can guide future studies.

Key words: microglia, proteomics, mass spectrometry, FACS, MACS

Background

Microglia are the resident macrophages and primary immune effectors in the brain and have become central to Alzheimer's disease (AD) biology. They were initially identified in AD brains surrounding plaques [1, 2], implicating them in the pathogenesis of AD, but whether microglia are protective [1, 2] or detrimental [3, 4] remains elusive. The more causal role of microglia in AD is evidenced by data from recent unbiased genome-wide association studies (GWAS) that have identified several single-nucleotide polymorphisms (SNPs) in immune related genes as independent risk factors for late-onset AD [5, 6]. Approximately two thirds of the 29 susceptibility genes are exclusively or most highly expressed in microglia, directly implicating microglia-mediated disease mechanisms in AD [5, 6].

Cell isolation and separation methods such as fluorescence activated cell sorting (FACS), magnetic activated cell sorting (MACS), differential centrifugation, and immunopanning are typically used to obtain a single-cell suspension of microglia from fresh mouse and human brain tissues [7-10]. Next generation RNA-sequencing has enabled the quantification of transcripts in low numbers of cells isolated from brain tissue. Transcriptome profiles of isolated microglia from animal models of AD have shown that as neurodegeneration progresses or at young and old ages, homeostatic microglia adopt transcriptionally distinct phenotypes and have heterogeneous transcriptomic signatures in different brain regions [11-16]. Though comprehensive transcriptomic analyses have proven useful in the characterization of microglia, there is still a gap in our understanding of what they mean biologically and how these transcriptional profiles relate to protein function. For instance, mRNA and protein expression profiles differ quantitatively, temporally, and spatially [17]. Several studies have shown that transcript-level and protein-level expression data are discordant because of post-transcriptional processes such as mRNA regulation, post-translational protein modifications, and protein recycling and degradation [18, 19]. Protein-mRNA correlation coefficients reach no higher than 0.47 in complex tissues like the brain and this relation is poorly understood in acutely isolated brain cell types including microglia [20]. Therefore, a global and comprehensive proteomic profiling of isolated microglia can make the most proximate assessment of their biological functions, rather than transcriptional profiling.

Proteomic studies of microglia have primarily used *in vitro* cultured or neonatal microglia [20-22] and few studies have used $CD11b^+$ MACS enrichment to obtain >90% microglia for downstream proteomic analyses. In an effort to elucidate proteomes of adult microglia, we have successfully performed quantitative tandem mass tag (TMT) mass spectrometry (MS) of acutely isolated $CD11b^+$ MACS-enriched microglia from adult (6-7mo) mice of normal, acute neuroinflammatory (lipopolysaccharide [LPS]-treatment), and chronic neurodegenerative (5xFAD model of AD) states [23]. This deep (4,133 proteins quantified) and comprehensive proteomic study of isolated mouse microglia allowed us to identify shared and unique microglial proteomic changes in AD mouse models and has given us insight into novel roles for microglial proteins in human neurodegeneration [23]. Importantly, this study emphasizes the value of applying state-of-the-art proteomics methods to resolve cell-type specific contributions to disease. However, despite high cell purity of MACS-enriched microglial isolates, these data also informed us that cell enrichment by MACS still suffers from contamination by proteins from other cell types. In support of this limitation, we found that despite >90% microglial cell enrichment, only 5% of the total proteins identified were actually enriched in microglia. Furthermore, we also found that astrocytic (Gfap) and oligodendrocyte (Mbp) proteins were still highly abundant in MACS-enriched proteomes. Therefore, optimization of microglia purification strategies that are best suited for microglial proteomic studies are warranted prior to comprehensive characterization in disease models as well as in human tissues. While both MACS-enriched and FACS-based cell purification yield high cell purity, protein-rich non-cellular elements can be definitively excluded by FACS, but not by MACS. In this study, we compared the proteomes of MACS-enriched and FACS-isolated $Cd11b^+$ microglia to characterize the purification efficiency of each technique. We find that overall,

both strategies effectively enrich microglia, but that FACS results in less background contamination of the proteome compared to MACS isolation.

Results

Differential expression and comparative analyses of MACS- vs. FACS-based enrichment

We obtained the proteomes of CD11b$^+$ microglia from 4-month-old male C57BL6/J wild-type mice (N = 10) isolated using two different strategies: magnetic activated cell sorting (MACS N = 5, >90% enrichment [23]) and fluorescence activated cell sorting (FACS, N = 5, average 30,000 total cells per sample). MACS-enriched and FACS-isolated microglia cell lysates in 8M urea were digested with LysC and Trypsin, labeled with isobaric multiplex tandem mass tags (TMT), and analyzed by synchronous precursor selection (SPS)-based MS3 (SPS-MS3) (**Figure 1D**). Due to the isobaric nature of the tags, all shared peptides from the 10 samples exhibit the same biochemical properties (i.e., exact mass, ionization efficiency, and retention time). Only during MS/MS does each tag fragment and release unique reporter ions, which are then used for peptide quantitation. Thus, one major advantage of multiplex TMT based quantification is that the peptides are pooled across all samples, which increases the precursor peptide signal in the mass spectrometer for proteins common to all samples by up to 10-fold (e.g. TMT 10-plex) when compared to running each sample individually by label-free quantification (LFQ). This is especially important when isolating small numbers of cells (~30,000) as in this study. In total, we identified 6,404 peptides mapping to 1,876 protein groups. Of these, 1,791 proteins were quantified in at least 3 of the 5 replicates in each group, and 4 demonstrated expression patterns unique to only the MACS-enriched group, of which we excluded 2 due to low protein FDR. A total of 953 proteins were differentially expressed ($p < 0.05$, Student's t test) comparing FACS and MACS microglial proteomes, and of these, 815 met significance thresholds at the FDR <5% level. Of the 953 differentially enriched proteins, 685 were increased and 268 proteins were decreased in abundance in the FACS microglia proteome. When we compared the relative abundance of the 685 significantly increased proteins, 36 proteins had a 2-fold or greater increase in abundance (**Figure 2A, solid red dots**) in the FACS proteome than in the MACS proteome (top 5: Apex, Fam3c, Lcn2, Lbr, S100a8). Of the 268 significantly decreased proteins, 65 proteins had a 2-fold or greater decrease in abundance in the FACS proteome (**Figure 2A, solid blue dots**), i.e., an increased abundance in MACS proteome (top 5: Gap43, Gpm6b, Sh3gl2, Psip1, Hmgn3). Gene Ontology (GO) analysis of proteins significantly increased (n = 685) in the FACS microglia proteome indicated an over-representation of proteins from "cytosolic", "endoplasmic reticulum (ER)", and "ribosome" cellular components, and proteins involved in processes such as "regulation of protein metabolic" and "immune system" (**Figure 2B**). The cytosolic and ER bias of the FACS proteome, argues against a nuclear proteomic bias of the FACS approach. Conversely, "mitochondrial" and "synaptic" proteins, and proteins involved in "electron transport chain", "neurotransmitter transport", and "synaptic transmission" processes were over-represented in the proteins significantly decreased in the FACS proteome (**Figure 2B**). These results show that despite using identical mass spectrometry approaches and high cellular purity obtained by MACS and FACS-based microglial enrichment approaches, the proteomes from each strategy are indeed very different. Namely, the proteome of MACS-enriched microglia appears to be heavily biased towards synaptic proteins, suggesting a significant neuronal component in these samples, while the FACS-isolated proteome is enriched for immune function, indicating higher enrichment of microglial proteins.

Microglial cell-type specific proteins are enriched in FACS isolated mouse microglia

In order to definitively assess the cellular level biases of FACS and MACS microglial proteomes, we performed cell-type enrichment analysis using protein marker lists derived from proteomes of four purified mouse brain cell-types — microglia, neurons, astrocytes, and oligodendrocytes (referred to as the "reference cell-type proteome") [20] (**Figure 3A**). At the time of this work, there was no existing reference for purified endothelial cell proteome. Of the 953 differentially expressed proteins in our entire dataset, 14.7% (140/953) of the proteins were microglial specific, while 22.1% (20/953) were neuronal, 3.5% (33/953) were astrocytic, and 2.4% (23/953) were oligodendrocyte cell-type specific proteins (**Figure 3A**). There were 77.3% (737/953) differentially enriched proteins that were not unique to any given cell-type, indicating that most cellular proteins even in distinct brain cell types, are shared (**Figure 3A, red dots**). In the FACS proteome, 98.3% (139/140) of microglial proteins were increased (**Figures 3B, top 20 proteins**) and 0.7% (1/140) proteins were significantly decreased compared to the MACS proteome (**Table 1**). Of the 20 neuronal cell-type proteins, 10% (2/20) were increased while 90% (18/20) of the proteins were decreased in abundance in the FACS microglia proteome (**Figure 3C; Table 1**). Lastly, 57.6% (19/33) astrocytic and 21.7% (5/23) oligodendrocyte cell-type specific proteins were significantly increased in FACS microglial proteome and 42.4% (14/33) astrocytic and 78.3% (18/23) oligodendrocyte proteins were significantly decreased in abundance in FACS microglia proteome compared to MACS microglia proteome (**Figure 3C; Table 1**). These data show that using a cell-type marker list from a reference cell-type proteome [20], our FACS-isolated proteome is significantly enriched with microglia-associated proteins and is depleted of neuronal, astrocyte, and oligodendrocyte proteins.

In addition to utilizing a reference cell-type proteome [20] to define cell-type protein markers in our FACS-isolated and MACS-enriched microglia proteomes, we analyzed the same data for cell-type enrichment with a marker list derived from RNAseq data of five purified mouse brain cells (termed "reference cell-type transcriptome") — microglia, neurons, astrocytes, oligodendrocytes, and endothelial cells [9] (**Supplemental Figure 2A**). Of the 953 differentially expressed proteins, 12.5% (119/953) of the proteins were microglial specific, while 5.2% (50/953) were neuronal, 1.7% (16/953) were astrocytic, 1.6% (15/953) were oligodendrocytic, and 3.2% (31/953) were endothelial cell-specific proteins (**Supplemental Figure 2A; Table 1**). There were 75.8% (722/953) of the 953 differentially expressed proteins that were not defined by a cell-type according to the reference cell-type transcriptome marker list (**Supplemental Figure 2A, open black dots**). Of the 119 identified microglial proteins (**Supplemental Figure 2A, red dots**), 100% of them were significantly enriched in the FACS microglia proteome compared to MACS microglia proteome (**Table 1**). For the other cell-types, 8% (4/50) of the neuronal, 43.8% (7/16) of the astrocytic, and 73.3% (11/15) of the oligodendrocyte specific proteins were increased in FACS-isolated microglia proteome (**Table 1**). Surprisingly, 93.5% (29/31) of the identified endothelial cell proteins were significantly enriched and 6.5% (2/31) of the proteins were decreased in FACS-isolated microglia proteome compared to the MACS-enriched microglia proteome (**Table 1**). In sum, using a reference transcriptome to define cell-type enrichment, we observed a similar trend where the FACS-isolated proteome was enriched with microglial proteins and depleted of neuron, astrocyte, and oligodendrocyte cell specific proteins. Surprisingly, we also observed an enrichment of endothelial markers in the FACS proteome.

Given that both references identified varying numbers of cell-type proteins (**Table 1**), we sought to determine whether the degree of overlap in the number of cell-type proteins identified by both cell-type enrichment strategies. If we considered the 140 microglia proteins defined by the reference cell-type proteome, ~73% (87/119) of them overlap with proteins defined to be microglial by the reference cell-type transcriptome (**Supplemental Figure 2B**). The reference cell-type proteome defined 20 proteins to be neuron specific, where ~20% (10/50) of the proteins overlapped with the neuronal proteins identified by the reference cell-type transcriptome (**Supplemental Figure 2B**). Additionally, the reference cell-type proteome defined 33 proteins to be astrocyte specific and 23 to be oligodendrocyte specific with ~44% (7/16) and ~27% (4/15) of

the proteins overlapping with the astrocyte and oligodendrocyte proteins defined by the reference cell-type transcriptome, respectively (**Supplemental Figure 2A**). To summarize, the two reference cell-type marker lists we used identified minimally overlapping and varying numbers of proteins for each cell-type.

To further confirm the validity of the apparent cellular biases of MACS vs. FACS proteomes in our dataset, we compared our results to our recently published MACS-based microglial proteome from wild-type mice and mouse models of AD in which 4,133 proteins were identified by TMT-MS in $CD11b^+$ MACS-enriched microglia [23]. In this secondary analysis (**Supplemental Figure 3**) we cross-referenced with the reference cell-type proteome [20] and found that 78.5% of all proteins did not map to a cell-type, while only 4.5% were microglial and 17% of the proteins were enriched in other cell-types. While microglia-specific proteins such as Msn and Cotl1 were highly abundant, neuronal proteins (Camk2a, Gap43), astrocyte proteins (Gfap, Aldoa) and oligodendrocyte proteins (Mbp) were also identified as highly abundant proteins (**Supplemental Figure 3B,** >90th percentile of relative abundance).

Collectively, these cell-type enrichment analyses of our proteomic data, integrated with existing reference brain cell type-specific proteomes and transcriptomes, clearly show that MACS-based proteomes are still contaminated by non-microglial proteins, while the FACS-based approach results in better enrichment of microglial proteins and depletion of neuronal and other glial proteins.

Comparative analysis of FACS isolated mouse microglial proteome and transcriptome reveals shared and unique microglial proteins

Although molecular profiling of microglia has been biased towards transcriptomic studies, proteins and not transcripts are the effectors of biological functions. Significant discordance between transcriptomic and protein level expression have also been shown [18]. A comparison of transcriptomic and proteomic expression in adult mouse microglia can reveal shared (concordant) molecular expression profiles, as well as highlight differences (discordance) between mRNA and protein levels in microglia. To characterize the concordance and discordance at transcript and protein expression levels in microglia, we integrated our proteomic findings from FACS-isolated microglia with existing RNAseq transcriptomic data of $CD11b^+$ microglia from 2-month-old wild-type mice, isolated using nearly-identical FACS-based approaches [8]. Relative abundance values (abundance percentile rank) of microglial proteins identified in our FACS-isolated mouse microglia dataset (n = 206) were binned into quartiles (Bins: 0-25, 25-50, 50-75, 75-100) and compared with the reference FACS-isolated microglia transcriptome. Of the 206 microglia specific proteins/gene symbols, ~21% (n = 44) were highly abundant in both datasets and the overall level of discordance (>50th percentile or <50th percentile in either dataset) was 40%. We found 90 proteins/gene symbols to be highly abundant (>50th percentile) in both datasets (**Figure 4A**, Q4), and among these, microglial proteins such as Hexb, Ctsd, Pfn1, Msn, Aif1 (Iba1), and many others, were present in the top 10th percentile of abundance in both datasets (**Figure 4A**, Q4 red dots). Consistent with our prior findings, Msn, Hexb, Pfn1, and Coro1a were also found to be highly abundant microglial proteins [9, 20]. Additionally, a novel microglial specific protein we previously have identified, Cotl1 [23], is also highly abundant in both datasets (**Figure 4A**, Q4). The first quadrant (Q1) has ~27 proteins/gene symbols that are low in both proteomic and reference RNAseq datasets (**Figure 4A**, Q1 black dots). The second quadrant (**Figure 4A**, Q2) represents proteins/gene symbols with high abundance in our proteomic dataset but low abundance in the reference RNAseq dataset. Q2 contains ~21 proteins/gene symbols, with Anxa5, S00a9, S100a8, and Hmga1 in the top 10th percentile of protein abundance (**Figure 4A**, red squares). The third quadrant (Q3) has ~62 proteins/gene symbols that display a low abundance in our proteomic dataset but a high abundance in the reference RNAseq dataset and includes proteins such as Bin1, Snx5, and Gpx1 in the top 10th percentile (**Figure 4A**, Q3 open

red dots). To summarize, we have defined a core set of highly-abundant microglial proteins in adult mice which can be used as indicators of microglial abundance in future proteomic studies. The results also highlight the clear discordance between transcript-level and protein-level expression in microglia.

Msn and Cotl1 are highly expressed by microglia in adult mouse brain

We identified 44 highly abundant proteins at the transcriptional and protein levels in FACS-isolated microglia (**Figure 4A, Q4**) and from these, we chose Msn and Cotl1 for additional neuropathological studies to characterize expression in the mouse brain. Moesin or Msn is a member of the ezrin-radixin-moesin (ERM) family of proteins that link the C-terminal domain of cortical actin filaments to the plasma membrane [24]. Msn is expressed ubiquitously in various cells such as macrophages, lymphocytes, fibroblastic, endothelial, epithelial, and neuronal cell lines [25-27]. Msn is highly expressed by microglia at the protein and transcript levels [8, 9, 20], consistent with our finding that Msn is a highly abundant microglial protein (Figure 4B). It is also highly expressed in endothelial cells at the transcript level [9]. We co-immunostained brains from 6-7 month old Cx3cr1$^{CreER\text{-}YFP}$ mice on wild-type (WT, N = 4) or 5xFAD (N = 6) backgrounds with antibodies against Msn and YFP/GFP. Cxc3cr1$^{CreER\text{-}YFP}$ mice display YFP immunofluorescence in Cx3cr1^{+} microglia in the brain [28, 29]. In Cxc3cr1$^{CreER\text{-}YFP}$-WT mouse cortex, we observed GFP immunofluorescence within the cell body and processes of ramified microglia (**Figure 4C**, arrow) and detected diffuse Msn immunofluorescence in the same ramified microglia (**Figure 4C**, arrowhead). We also observed Msn immunofluorescence in non-microglial cells which resembled endothelial cells (**Figure 4C**, asterisk), consistent with previously reported Msn expression in endothelial cells [9]. In Cxc3cr1$^{CreER\text{-}YFP}$-5xFAD mouse cortex, we observed a marked activated morphology of GFP immunofluorescent microglia and found strong co-localization of GFP- and Msn-positive microglia surrounding dense Aβ plaques (**Figure 4C**, circle).

The second protein we validated was Cotl1, which we have previously identified as a novel microglia-specific marker from a quantitative TMT-MS proteomic analysis of MACS-enriched CD11b^{+} microglia from adult mice in normal, acute neuroinflammatory, and chronic neurodegenerative states (5xFAD model of AD) [23]. Cotl1 or coactosin like F-actin binding protein 1 is an actin-binding protein expressed by immune cells including macrophages and has been recently reported to regulate actin dynamics at the immune synapse [30, 31]. Furthermore, Cotl1 is highly and specifically expressed by microglia at the transcript and protein levels [9, 20]. In the current study, we were able to replicate our previous finding of Cotl1 as a microglial marker with a significantly higher abundance (1.4-fold higher, p = 0.001) in the FACS proteome than MACS proteome. We co-immunostained the same brains from Cx3cr1$^{CreER\text{-}YFP}$ mice on WT or 5xFAD backgrounds for Cotl1 and YFP/GFP. In the Cxc3cr1$^{CreER\text{-}YFP}$-WT cortex, Cotl1 immunofluorescence was specifically detected in GFP immunofluorescent microglia (**Figure 4D**, arrow). Qualitatively, there was an increase in the number of microglia co-expressing GFP and Cotl1 in the Cxc3cr1$^{CreER\text{-}YFP}$-5xFAD mouse cortex (**Figure 4**, asterisk). The microglia in the Cxc3cr1$^{CreER\text{-}YFP}$-WT cortex appeared ramified, but those in Cxc3cr1$^{CreER\text{-}YFP}$-5xFAD cortex adopted an activated morphology with shorter swollen processes and larger cell bodies (**Figure 4D**).

These results show that proteomic analysis of FACS-isolated microglia yields highly abundant microglial specific proteins, such as Msn and Cotl1, that are also high in abundance at the transcript level which can serve as markers of microglia in the mouse brain at normal and disease states.

Dicussion

Bioinformatic studies of human brain gene and protein expression have consistently identified microglial genes/proteins within immune pathways as determinants of disease progression and cognitive decline [5, 32, 33]. Molecular characterization of microglia has been traditionally biased towards transcriptomic studies [34-36] rather than proteomic studies due to the generally low protein yield from isolated cells, challenges related to microglial isolation from the brain, and technical requirements for mass spectrometry analyses. Multiple studies have shown the discordance between transcript-level and protein-level expression data attributed to post-transcriptional processes such as post-transcriptional mRNA regulation, post-translational protein modifications, protein recycling and degradation [17-19]. Therefore, comprehensive profiling of proteins, rather than transcripts, of microglial cells is necessary for a deeper understanding of microglia-mediated disease mechanisms in neurodegenerative diseases such as AD.

Prior proteomic studies have consistently used magnetic-activated cell sorting (MACS) enrichment strategies to isolate microglia from fresh mouse or human brain [20, 23, 37]. MACS-enrichment aims to facilitate a rapid, high-throughput, immuno-magnetic separation of a pure population of a desired cell-type, i.e. microglia, from a single cell-suspension; however, it is limited by low yield and contamination by non-microglial proteins despite high cellular purity. In the current study, we aimed to determine whether a fluorescence activated cell sorting (FACS)-isolation strategy overcomes these limitations by performing the first comprehensive proteomic comparison of MACS-enrichment and FACS-isolation strategies for acutely-isolating microglia from adult (4 month old) mouse brains. The proteomes obtained by each isolation strategy are surprisingly very different: the MACS-enriched microglia proteome overrepresents synaptic proteins, suggesting a significant neuronal component in these samples, while the FACS-isolated microglia proteome is enriched for immune function proteins, indicating higher enrichment of microglial proteins. In order to assess whether the FACS proteome was indeed enriched for microglial proteins, we performed cell-type enrichment analysis of the differentially expressed proteins between the MACS and FACS proteomes and demonstrated that the FACS-isolation approach, when coupled with TMT-MS, is a superior method yielding a proteome that is highly enriched for canonical microglia-specific proteins while non-microglial proteins, particularly those derived from neurons and oligodendrocytes, are significantly depleted.

A strength of our study is the use of TMT-MS for quantitative proteomic characterization. The multiplex paradigm enables the accurate quantitation of thousands of proteins across many samples simultaneously for large-scale quantitative proteomic applications [38, 39]. Also, a major advantage of TMT-MS is the ability to multiplex all of the peptide sets prepared from multiple samples to be combined into a single LC-MS/MS analysis, resulting in improved breadth of coverage by avoiding missing values that are common in label-free based quantification [40, 41]. The combination of TMT-MS and SPS-MS3 methods significantly improved the acquisition, quantitation, and depth of MACS-enriched and FACS-isolated microglial proteomes. Critically, collapsing the 10-TMT channels (5 samples/isolation strategy) resulted in higher signals and identified proteins, overcoming the challenges of low protein yield typically expected from isolation of rare cell-types such as microglia. Many studies pool isolated microglia from 3-12 mouse brains for a MS run to increase protein yield and improve detection/quantitation of proteins in a MS run [9, 20, 23]; however, each sample in our study consisted of microglial cells isolated from one whole mouse brain without pooling for either isolation strategy. This is significant because 1) we demonstrate that at least 18,000 FACS-isolated microglial from one mouse brain is sufficient for a thorough proteomic analysis, 2) sampling bias is minimized when samples are not pooled, and 3) this method is especially cost-effective for complex, long-term mouse studies. The limitations of our approach are also made apparent by the aforementioned points. We identified approximately 1,800 proteins compared to the 4,133 proteins identified in our previous proteomic analysis of acutely isolated microglia [23]. This low number of identified proteins could have been ameliorated by pooling brain samples, as this significantly increases our protein yield. Additionally, enzymatic digestion rather than mechanical dissociation of brain tissue prior to isolation could

increase microglial cell yield from one whole brain, and thus, protein yield. Last, this could be attributed to non-cellular contamination in the MACS samples that were combined with FACS samples for TMT-MS.

Our study also supports the use of our validated pipeline of FACS-based isolation coupled with TMT-MS for characterization of non-microglial brain cell types. One advantage of the FACS approach is it provides the opportunity to isolate other cell-types from the brain, which is not feasible using MACS approaches without compromising cell integrity and viability. In our current study, we did not perform enzymatic digestion of the brain to maximize microglial enrichment prior to FACS or MACS. However, enzymatic digestion can significantly increase the yield of endothelial cells as well as other glial cells (astrocytes and oligodendrocytes), allowing simultaneous cell type isolation by FACS. A cell isolation methodology termed concurrent brain cell type acquisition (CoBrA) has been used to isolate microglia, endothelial cells, astrocytes, and oligodendrocytes from mouse brain for RNAseq studies [42]. Unlike transcriptomic strategies, proteomic applications require specific strategies to reduce protein contamination from serum, albumin, and other proteins such as keratin, which we are currently optimizing for an analogous simultaneous cell-type isolation pipeline for proteomic studies. Based on our demonstration of feasibility in obtaining high-quality proteomes from FACS-isolated microglia, which traditionally have very low protein yield per cell, our results support the feasibility of using FACS to isolate distinct cell types with high purity while minimizing non-specific contamination, for simultaneous proteomic characterization of multiple cells types. This is particularly important for resolving why we observed a significant enrichment of endothelial genes/proteins in our FACS-isolated microglial proteome, which could mainly be a reflection of our cell-type enrichment analysis method for endothelial cells. Current brain endothelial cell biology is solely based on expression at the transcript level because no purified endothelial proteomes exist, thus, our cell-type enrichment analysis was conducted using a mouse brain cell-type transcriptomic reference [9]. Given the discordance between transcript-level and protein-level expression, it is difficult to conclude that there is indeed endothelial cell-type protein enrichment by FACS targeting microglial enrichment. This can only be resolved by proteomic characterization of concurrently isolated microglial cells and endothelial cells from the same mouse brain and comparison of these data with existing endothelial transcriptomic data.

We assessed our MACS- and FACS- microglial proteomes for cell-type enrichment with two different mouse brain cell-type reference datasets: cell-type resolved proteome by Sharma *et al.* [20] and cell-type resolved transcriptome by Zhang *et al*. [9] Although, both reference datasets identified the FACS-proteome to be enriched with microglial proteins/gene symbols and depleted of non-microglial proteins/gene symbols, there were still a significant number of gene products that were not assigned to a specific cell-type. This could be attributed to several factors. First, it could be that these proteins/genes are ubiquitous in the brain regardless of the cell-type. Second, there are inherent differences in the isolation methodologies between our study and the reference studies. For example, the refence cell-type proteome [20] isolated cells using MACS-enrichment and primary cell-culture [20], while the reference cell-type transcriptome [9] performed FACS isolation from transgenic mice and immunopanning to isolate cells. Lastly, the expression or regulation of these proteins/gene symbols in their respective cell-type might vary with age. We characterized the microglial proteome of adult mice, while both reference datasets characterized microglia and other brain cell-types from vastly younger mice ranging in age from P1 to P8* [9, 20]. In summary, the combination of all these factors may have limited our ability to fully resolve the cell-type origin of the proteins identified within our dataset and highlights the need for comprehensive characterization of the proteome or transcriptome of mouse brain cell-types using consistent mouse models at similar ages, isolation protocols, and technical and analytical measures that will allow for cross-study comparisons.

We contrasted our FACS-isolated microglial proteome with a reference FACS-microglial transcriptome by Bennet *et al.* [8], and identified two highly abundant microglia specific proteins,

Msn and Cotl1, in our FACS-isolated microglial proteome that are also high in abundance at the transcript level [8]. Our immuno-histochemical studies show that Msn and Cotl1 proteins, like known other markers such as Tmem119 or Iba1, could serve as novel markers of microglia in the mouse brain in normal and disease states. In WT mice, Msn was expressed in ramified/homeostatic microglia as well as non-microglial cells that resembled endothelial cells, consistent with prior transcriptomic studies showing that Msn is also highly abundant in endothelial cells [9]. Furthermore, in the 5xFAD mouse brains, Msn protein expression was localized to large clusters of reactive microglia rather than ramified microglia, specifically within microglial processes that surround and infiltrate Aβ plaques. Consistent with ezrin-radixin-moesin proteins, the pattern of Msn expression in microglia appeared to be more membrane localized rather than cytosolic [43]. We also validated a protein we previously identified as a microglial marker, Cotl1, through MACS-enrichment microglial proteomic analysis [23]. Cotl1 protein expression was observed in microglia of WT and 5xFAD brains, with higher immunofluorescence and increased microglial size observed in the 5xFAD mice only. Overall, our findings suggest that proteomic characterization of FACS-isolated microglia does indeed identify strong microglia-specific markers such as Msn and Cotl1 that can be used to detect both ramified and Aβ plaque-associated microglia in the mouse brain, but there is still a discordance between protein-level and transcript-level expression in microglia. We identified proteins/gene symbols with high abundance in our FACS proteome dataset which are low at the transcript-level, as well as proteins/gene symbols with low abundance in our FACS proteome, but that are high at transcript level. One can argue that this discordance is due to comparison of unmatched samples, however, the reference dataset we used for our comparative analysis is the closest in terms of isolation methodology and age of mice the microglia were isolated from, allowing for a relatively fair comparison between our proteome and their transcriptome [8]. One way to better estimate protein-transcript correlations is by concurrently measuring proteins and transcripts within identical microglia samples. This would deepen our insight into intra-microglial heterogeneity and complexity in normal and disease states.

Conclusion

This study establishes FACS isolation, rather than MACS enrichment, as a valid and preferred approach for future quantitative proteomic studies of adult mouse microglia using disease models.

Methods

Animals

Mice were housed in the Department of Animal Resources at Emory University under a 12-hour light/12-hour dark cycle with ad libitum access to food and water. All procedures were approved by the Institutional Animal Care and Use Committee of Emory University and were in strict accordance with the National Institute of Health's "Guide for the Care and Use of Laboratory Animals."

Acute isolation of CD11b-positive microglia

Male 4-month-old C57Bl/6J mice (N = 10) were anesthetized with isoflurane, followed by exsanguination and cardiac perfusion with 30mL of ice-cold 1× phosphate buffered saline (1×PBS). The brain was immediately dissected and mechanically homogenized over a 40µm cell strainer. Subsequently, the homogenate was centrifuged for 5min at 800×*g* at room temperature (RT), supernatant was carefully decanted, and pellet was resuspended in 6mL of 35% stock isotonic Percoll (SIP) solution diluted with 1×HBSS (SIP: nine parts 100% Percoll and 1 part 10× HBSS). The cell suspension was transferred to a new 15mL conical and 3mL of 70% SIP was slowly underlaid. The established gradient was centrifuged for 25min at 800×*g* with no brake at

15ºC. The top floating myelin layer was aspirated and 3mL from the 35-70% interphase, containing the mononuclear cells (**Figure 1A**), was collected without disturbing the 70% layer. The mononuclear cells were washed with 6mL of 1×PBS, centrifuged for 5min at 800×*g*, and cell pellet was resuspended in 100µl of 1×PBS.

Isolated mononuclear cells from five brains were then further purified by CD11b positive selection using MACS columns (*N* = 5 mice, >90% enrichment of $CD11b^+$ microglia [23]) (Miltenyi Biotec, Cat# 130–093-636) to selectively enrich microglia and brain mononuclear phagocytes (**Figure 1A**). Mononuclear cells from the remaining five brains were labeled with APC-Cy7 rat anti-CD11b antibody (BD Pharmingen, Cat# 557657) for 30min at RT and sorted using a BD FACSAria II cell sorter (**Figure 1B**). In order to allow for a fair comparison between both approaches, we intentionally FACS-isolated $CD11b^+$ myeloid cells (predominantly microglia) rather than using a $CD11b+CD45^{int}$ selection strategy. Since live/dead gating is not feasible for MACS-enrichment, we intentionally did not use live/dead exclusion in the gating strategy for FACS. However, we confirmed in independent experiments that cell viability using our FACS strategy is >95% within $CD11b^+$ microglia. We have also previously shown that $CD45^{high}$ brain-infiltrating macropahges represent <5% of cells within $CD11b^+$ brain myeloid cells [23], and therefore, MACS-enriched or FACS-isolated $CD11b^+$ brain myeloid cells are referred to as microglia in this manuscript.

Cell homogenization and protein digestion

Isolated microglia were lysed in 200µL of lysis buffer (8M urea, 100mM $NaHPO_4$, pH 8.5) with HALT protease and phosphatase inhibitor cocktail (ThermoFisher, Cat. No. 78446) and each sample was sonicated for 3 cycles consisting of 5 seconds of active sonication at 30% amplitude followed by 15 seconds on ice. Protein concentration was determined by bicinchoninic acid (BCA) assay (Pierce, Cat. No. 23225). Protein digestion was performed as previously described [40]. Briefly, 6µg of protein for each sample was reduced with 1mM dithiothreitol (DTT) at room temperature for 30 min and alkylated by 5mM iodoacetamide (IAA) in the dark for 30 min. Samples were then diluted (8-fold) with 50mM triethylammonium bicarbonate (TEAB), digested overnight with Lysyl endopeptidase (Wako, Cat. No. 127-06621) at 1:100 (w/w). The peptide solutions were acidified to a final concentration of 1% formic acid (FA) and 0.1% triflouroacetic acid (TFA), desalted with a C_{18} Sep-Pak column (Waters, Cat. No. WAT054945) and dried down in a vacuum centrifuge (SpeedVac Vacuum Concentrator).

Tandem mass tag (TMT) labeling of peptides was performed according to manufacturer's instructions and as previously described [40]. One batch of 10-plex TMT kit (Thermo Fisher, Cat. No 90110) was used to label all ten samples (**Figure 1C**). All ten channels were then combined and dried in a vacuum centrifuge.

High pH reversed-phase peptide fractionation

High pH reversed-phase peptide fractionation kit was used to perform desalting and fractionation as per manufacturer's protocol (ThermoFisher, Cat. No. 84868). Briefly, the dried sample containing all ten TMT channels was reconstituted with 300µL of 0.1% trifluoroacetic acid (TFA) and added to conditioned reversed-phase fractionation spin columns containing 20mg of resin in a 1:1 water/DMSO slurry. A sequential gradient of increasing acetonitrile (ACN) concentrations in a high-pH elution solution (0.1% triethylamine) was applied to the columns to elute bound peptides into 9 different fractions collected by centrifugation at 3000×*g*. Each fraction was dried in a vacuum centrifuge and stored at 4 degrees until mass spectrometry.

Mass spectrometry analysis and TMT data acquisition

Assuming equal distribution of peptide concentration across all 9 fractions, 10µL of loading buffer (0.1% TFA) was added to each fraction and 2µL was separated on a 25 cm long by 75 µm internal diameter fused silica column (New Objective, Woburn, MA) packed in-house with 1.9 µm Reprosil-

Pur C18-AQ resin. The LC-MS/MS platform consisted of a Dionex RSLCnano UPLC coupled to an Orbitrap Fusion mass spectrometer with a Flex nano-electrospray ion source (Thermo Fisher). Sample elution was performed over a 120 min gradient with a constant flow rate of 300nl/min. The gradient consisted multiple steps starting at 3% and going to 7% Buffer B (0.1% formic acid in ACN) over 5 mins, from 7 to 30% B over 80 mins, from 30 to 60% over 5 mins, from 60 to 99 over 2 mins, constant at 99% for 8 mins and immediately back to 1% for 20 mins. The mass spectrometer was operated in positive ion mode and utilized the synchronous precursor selection (SPS)-MS3 method for reporter ion quantitation as described [40] with a top speed cycle time of 3 seconds. The full scan range was 400–1500 m/z at a nominal resolution of 120,000 at 200 m/z and automatic gain control (AGC) set to 4 ×10^5. Tandem MS/MS Collision-induced dissociation (CID) spectra were collected in the ion trap with normalized collision energy set to 35%, max injection time set to 35 ms and AGC set to 1x10^4. Higher energy collision dissociation (HCD) synchronous precursor selection (SPS)-MS3 of the top 10 product ions at 65% normalized collision energy (CE) were collected in the orbitrap with a resolution of 60,000, a max injection time of 100 ms and an AGC setting of 5x10^4.

Protein identification and quantification

Raw files from Orbitrap Fusion were processed using Proteome Discover (version 2.1) and MS/MS spectra were searched against UniProt Mouse proteome database (54,489 total sequences) as previously reported [23]. SEQUEST parameters were specified as: trypsin enzyme, two missed cleavages allowed, minimum peptide length of 6, TMT tags on lysine residues and peptide N-termini (+229.162932 Da) and carbamidomethylation of cysteine residues (+57.02146 Da) as fixed modifications, oxidation of methionine residues (+15.99492 Da) and deamidation of asparagine and glutamine (+0.984 Da) as a variable modification, precursor mass tolerance of 20 ppm, and a fragment mass tolerance of 0.6 Da. Peptide spectral match (PSM) error rates were determined using the target-decoy strategy coupled to Percolator [44] modeling of true and false matches. Reporter ions were quantified from MS3 scans using an integration tolerance of 20 ppm with the most confident centroid setting. An MS2 spectral assignment false discovery rate (FDR) of less than 1% was achieved by applying the target-decoy strategy. Following spectral assignment, peptides were assembled into proteins and were further filtered based on the combined probabilities of their constituent peptides to a final FDR of 1%. In cases of redundancy, shared peptides were assigned to the protein sequence with the most matching peptides, thus adhering to principles of parsimony. The search results and TMT quantification as well as raw LC-MS/MS files are included in the ProteomeXchange online repository with identifier PXD015652. We included proteins with TMT abundance values in at least 3 of the 5 replicates per group, as well as proteins present within all 5 replicates in one group and absent in the other group (present only in MACS: total $n = 4$), but also display a high protein FDR confidence ($n = 2$, Gpm6b & Sh3gl2). Additionally, even though TMT labeling limits missing values, normalized abundances of zero were imputed as the lowest TMT abundance value in the dataset.

Gene ontology enrichment analysis

Gene Ontology (GO) functional annotation of differentially expressed proteins was performed using GO-Elite 1.2.5 as previously published [32, 33], with a minimum of five genes per ontology, meeting Fisher exact significance of $p < 0.05$, i.e., a Z-score greater than 1.96. The background gene list for GO-Elite consisted of total proteins identified and quantified in our dataset ($n = 1791$). Input lists included proteins that were significantly differentially expressed ($p < 0.05$ by Student's t-test, unadjusted) and with a ≥2-fold-change in abundance comparing FACS-microglia with MACS-microglia proteomes (**Supplemental Table 2**)

Differential expression analysis

Differentially enriched or depleted proteins (unadjusted $p \leq 0.05$) were identified by Student's t-test comparing the five FACS-isolated microglia samples and the five MACS-enriched microglia samples. Differential expression (FACS/MACS) is presented as volcano plots which display all proteins that either arise from expression of one of the proteins or genes in the cell type-specific enrichment lists [9, 20]. Significance of differentially expressed proteins was assessed using the one tailed Fisher's exact test and corrected for multiple comparisons by the FDR (Benjamini-Hochberg) method (**Supplemental Table 1**).

Cell-type enrichment analysis

Cell-type enrichment was performed by cross-referencing the number of differentially expressed proteins in our FACS vs. MACS microglial proteomes with cell type-specific gene lists from mass-spectrometry based proteomics [20] (termed "reference cell-type proteome") and RNA-Seq [9] (termed "reference cell-type transcriptome) of the following isolated mouse brain cell types: microglia, oligodendrocytes, astrocytes, neurons, and endothelial cells. Methods for determining cell-type enrichment of each protein or gene have been previously published and used in prior proteomic analyses [32, 45]. Of note, purified mouse endothelial proteomes have yet to be published.

Isolated microglial transcriptomics

We obtained and existing RNAseq transcriptome dataset from $CD11b^{+}$ microglia isolated by FACS from 2-month-old wild-type mice, Bennet *et al.* [8], and contrasted differentially expressed genes in this "FACS-isolated microglia transcriptome" with observed differentially expressed proteins in our FACS-isolated microglia. This dataset was selected because it enables the best comparison of transcriptomes and proteomes of microglia that were acutely isolated by FACS from adult wild-type mice, using nearly-identical approaches [8].

Immunofluorescence staining

Brains were isolated from wild-type $Cx3cr1^{CreER\text{-}YFP}$ mice ($N = 4$; Jackson Stock No. 021160) and $Cx3cr1^{CreER\text{-}YFP}$ mice crossed with 5xFAD mice ($N = 6$) at 6-7 months of age. $Cx3cr1^{CreER\text{-}YFP}$ mice constitutively express YFP in microglia. Briefly, the mice were anesthetized with isoflurane and perfused transcardially with 20mL of 1×PBS. The brains were immediately removed and hemisected along the sagittal midline. The left hemisphere was immersion-fixed in 4% paraformaldehyde for 24 hours, washed 3 times with 1×PBS, and transferred to 30% sucrose for another 24 hours. Subsequently, the brains were cut into 30µm thick sagittal sections using a cryostat. For immunofluorescence staining, 3-4 brain sections from each mouse were thoroughly washed to remove cryopreservative, blocked in 8% normal horse serum diluted in 1×TBS and 0.1% Triton-X for 1 hour, and incubated with primary antibodies diluted in 1×PBS overnight (1:200 goat anti-GFP [Rockland, Cat. No. 600-101-215], 1:100 rabbit anti-Msn [Abcam, Cat. No. ab52490], 1:100 rabbit anti-Cotl1 [Sigma-Aldrich, HPA008918]). Following washes and incubation in the appropriate fluorophore-conjugated secondary antibody (1:500, goat-FITC, anti-rabbit Rhodamine-red) for 30 min, sections were mounted on slides with mounting media containing DAPI for nuclear staining (Fluoreshield, Sigma-Aldrich F6057). Representative images of the same region in the cortex were taken using the Leica SP8 multi-photon confocal microscope and all images processing was performed using Fiji software [46].

Declarations

Ethics approval and consent to participate
Approval from the Emory University Institutional Animal Care and Use Committee was obtained prior to all animal-related studies (IACUC protocol # PROTO201800252).

Consent for publication
All authors have approved of the contents of this manuscript and provided consent for publication.

Availability of data and materials
The mass spectrometry proteomics data have been deposited to the ProteomeXchange Consortium via the PRIDE partner repository with the dataset identifier PXD015652.

Competing interests
The authors declare that they have no competing interests.

Funding
Research reported in this publication was supported by the National Institute on Aging of the National Institutes of Health (Award No. F32AG064862 to S.Rayaprolu); Alzheimer's Association (Award no. 37102 to S.Rangaraju); NINDS (Award no. K08-NS099474–1 to S.Rangaraju); Emory Neuroscience NINDS Core facilities (P30 NS055077); Alzheimer's Association (Award no. 11060 to NTS); Emory Alzheimer's Disease Research Center Grant (Award no. P50 AG025688). Other NIH grants that supported this work include U01AG046161, RF1AG057471, R01AG057330 and RF1AG057470, 5R01AG053960.

Authors' contributions
Conceptualization: NTS, S.Rangaraju. Methodology: S.Rayaprolu, TG, HX, S.Ramesha, DMD, EBD. Investigation: S.Rayaprolu, NTS, S.Rangaraju. Writing-Original draft: S.Rayaprolu, NTS, S.Rangaraju. Writing-Review and Editing: TG, HX, S.Ramesha, DMD, EBD, JJL, AIL. Funding Acquisition: S.Rayaprolu, NTS, S.Rangaraju. Resources: AIL, JJL, NTS, S.Rangaraju. Supervision: NTS, S.Rangaraju

Acknowledgements
Research reported in this publication was supported in part by the Emory Flow Cytometry Core (EFCC) and Emory University Integrated Cellular Imaging (ICI) Microscopy Core, two of the Emory Integrated Core Facilities (EICF). EFCC is subsidized by the Emory University School of Medicine and additional support was provided by the National Center for Georgia Clinical & Translational Science Alliance of the National Institutes of Health under Award Number UL1TR002378. ICI Microscopy core is subsidized by the Emory University Integrated Cellular Imaging Microscopy Core of the Emory Neuroscience NINDS Core Facilities grant, 5P30NS055077. The content is solely the responsibility of the authors and does not necessarily reflect the official views of the National Institute of Health.

Table 1. Summary of cell-type enrichment in differentially expressed proteins between MACS and FACS isolated microglia proteomes.

Reference	Cell type	Increased in FACS n (%)	Decreased in FACS n (%)	Total n
Reference cell-type proteome Sharma *et al*. 2015	**No cell-type**	520 (70.6)	217 (29.4)	737
	Microglia	139 (99.3)	1 (0.7)	140
	Neuron	2 (10)	18 (90)	20
	Astrocyte	19 (57.6)	14 (42.4)	33
	Oligodendrocyte	5 (21.7)	18 (78.3)	23
Reference cell-type transcriptome Zhang *et al*. 2014	**No cell-type**	515 (71.3)	207 (28.7)	722
	Microglia	119 (100)	0	119
	Neuron	4 (8)	46 (92.0)	50
	Astrocyte	7 (43.8)	9 (56.2)	16
	Oligodendrocyte	11 (73.3)	4 (26.7)	15
	Endothelial cell	29 (93.5)	2 (6.5)	31

FIGURE LEGENDS:

Figure 1. Study design and analytic approach for comprehensive quantitative proteomic analysis of isolated mouse microglia. A Work flow summarizing isolation and purification of $CD11b^+$ brain immune cells from 4-month-old male C57BL6/J wild-type mice (*N* = 10). Following mechanical dissociation of fresh, whole mouse brians and percoll density centrifugation, mononuclear cells were enriched for $CD11b^+$ microglia cells by magnetic activating cell sorting (MACS, *N* = 5 mice) or isolated via fluorescent activated cell sorting (FACS, *N* = 5 mice). **B** Representative flow cytometry gating strategy and antibody separation using CD11b-APC/Cy7 antibody for isolation of microglia. **C** Proteomic work flow for tandem mass tag (TMT) mass spectrometry (MS) based quantification. All 10 microglia samples were lysed in 8M urea, digested with LysC and Trypsin, and peptides were labeled using one 10-plex TMT kit. A total of 5 individual MACS-enriched microglia samples were dedicated to the first five channels (126, 127N, 127C, 128N, 128C) and 5 individual FACS-isolated microglia samples were dedicated to the last five channels (129N, 129C, 130N, 130C, 131). After labeling, the samples were combined and fractionated by off-line high pH fractionation (*n* = 9 fx total). Each fraction was analyzed and quantified by synchronous precursor selection (SPS)-MS3 on an Orbitrap Fusion mass spectrometer. **D** Analytic approach used for differential expression, cell-type enrichement, and comparative analyses of current proteomic dataset.

Figure 2. **FACS-isolated and MACS-enriched microglia proteomes are different. A** Scatter plot displaying relative abundance of all differentially expressed proteins (*n* = 953) between FACS-isolated microglia proteome and MACS-enriched microglia proteome (all dots represent $p < 0.05$). Red indicate proteins significantly higher in FACS proteome. Blue dots indidate proteins significantly higher in MACS proteome. Dotted lines differentiate proteins with a Log_2 fold change greater than 2 (solid red and blue dots). **B** Results from Gene Ontology (GO) enrichment analysis of 953 differentially expressed proteins against a background list of total proteins (*n* = 1791) idenfied in current dataset. Representative GO terms (top 5) from each of the three GO groups (peach: cellular component, blue: molecular function, dark green: biological process) are shown. Degree of enrichment of each GO term is indicated by the Z-score (X-axis). Vertical red line indicates an enrichment Z-score of 1.96.

Figure 3. Enrichment of microglia-specific proteins and depletion of non-microglial proteins by FACS. A Volcano plot displaying the distribution of differentially expressed proteins between FACS-isolated and MACS-enriched microglia proteomes with cell type-specific markers defined by a reference proteome [20] shows significant enrichment of microglial specific proteins in the FACS proteome ($p > 0.05$, Student's t test). Red dots = microglia, turquoise dots = neuron, pink dots = astrocyte, yellow dots = oligodendrocyte. Open black dots represent proteins with no cell-type marker identification. Grey dots represent differentially expressed proteins with a $p < 0.05$. Log_2 fold-change is shown on the X-axis, $-Log_{10}$(*p*-value) is shown on the Y-axis, and horizontal dotted line indicates $p = 0.05$. **B** Histogram displaying top 20 differentially expressed microglial proteins in FACS-isolated microglia proteome (red solid bars) and MACS-enriched microglia proteome (open red bars). **C** Histograms displaying top differentially expressed neuron, astrocyte, and oligodendrocyte cell-type proteins in FACS-isolated microglia proteome (solid bars) compared to same protein abundances in MACS-enriched microglia proteome (open bars). The X-axis shows list of proteins, Y-axis shows Log_2-transformed normalized abundance (abundance/row geomean), and error bars represent ± SEM.

Figure 4. Comparative analysis of FACS-isolated microglia proteome and transcriptome. A Scatter plot representation of the most abundant microglial proteins (defined by reference cell-type proteome, Sharma *et al.* [20]) identified in our proteome and the reference FACS-isolated

microglia transcriptome [8]. Proteins that were among the top 10th percentile of abundance in both datasets are highlighted in red dots in quadrant 4 (Q4), proteins that were among the top 10th percentile in reference transcriptome dataset are highlighted in open red dots in quadrant 3 (Q3), and proteins that were among the top 10th percentile in our proteomic dataset are highlighted in open red squares in quadrant 2 (Q2). **C** Representative images of Cx3cr1$^{CreER\text{-}YFP}$-WT (*N* = 4) and Cx3cr1$^{CreER\text{-}YFP}$-5xFAD (*N* = 6) mouse cortex stained with Msn (arrowhead and asterisk) and GFP (arrow) antibodies. Circle indicates Aβ plaque. **D** Representative images of Cx3cr1$^{CreER\text{-}YFP}$-WT (*N* = 4) and Cx3cr1$^{CreER\text{-}YFP}$-5xFAD (*N* = 6) mouse cortex stained with Cotl1 and GFP antibodies. Arrow and asterisk indicate overlap of GFP and Cotl1 immunofluoresence in the same microglia. Scale bar = 30µm.

Supplemental Figure 1. Viability of mechanically dissociated mouse brain mononuclear cells. Representative flow cytometry data displaying isolation of >95% live CD11b^{+} microglia from mechanically dissociated fresh, whole mouse brian (*N* = 4) following percoll density centrifugation.

Supplemental Figure 2. Enrichment of microglial and endothelial specific proteins by FACS. A Volcano plot displaying the distribution of differentially expressed proteins between FACS-isolated and MACS-enriched microglia proteomes with cell-type enricment defined by a reference cell-type transcriptome [9] shows significant enrichment of microglial and endothelial specific proteins in the FACS proteome ($p > 0.05$, Student's t test). Red dots = microglia, turquoise dots = neuron, pink dots = astrocyte, yellow dots = oligodendrocyte, green dots = endothelial cell. Open black dots represent proteins with no cell-type marker identification. Grey dots represent differentially expressed proteins with a $p < 0.05$. Log_2 fold-change is shown on the X-axis, -Log_{10}(*p*-value) is shown on the Y-axis, and horizontal dotted line indicates $p = 0.05$. **B** Minimal overlap in number of similar proteins identified by either reference cell-type proteome, Sharma *et al.* [20], or reference cell-type transcriptome, Zhang *et al.* [9].

Supplemental Figure 3. Contamination of non-microglial proteins in MACS-enriched microglia proteome. **A** Only 4.5% of the 4,133 quantified proteins are microglial specific [23] while nearly 17% of the proteins are from other cell types. **B** Highly-abundant proteins in our previous microglial proteomic study [23] included non-microglial proteins such as Mbp, Aldoa, Gfap, and Camk2a. Micro = microglia, Neu = neuron, Astro = astrocyte, Oligo = oligodendrocyte.

Supplemental table 1. Quantitative protein expression data from MACS-enriched and FACS-isolated mouse microglia. Log_2 transformed protein abundance data and differential expression analysis.

Supplemental table 2. GO Elite analysis of 953 significantly differentially expressed proteins between MACS-enriched and FACS-isolated mouse microglia proteomes.

References Cited

1. Griffin WS, Stanley LC, Ling C, White L, MacLeod V, Perrot LJ, White CL, 3rd, Araoz C: **Brain interleukin 1 and S-100 immunoreactivity are elevated in Down syndrome and Alzheimer disease.** *Proc Natl Acad Sci U S A* 1989, **86:**7611-7615.

2. Perlmutter LS, Barron E, Chui HC: **Morphologic association between microglia and senile plaque amyloid in Alzheimer's disease.** *Neurosci Lett* 1990, **119:**32-36.

3. Heneka MT, Carson MJ, El Khoury J, Landreth GE, Brosseron F, Feinstein DL, Jacobs AH, Wyss-Coray T, Vitorica J, Ransohoff RM, et al: **Neuroinflammation in Alzheimer's disease.** *Lancet Neurol* 2015, **14:**388-405.

4. Sarlus H, Heneka MT: **Microglia in Alzheimer's disease.** *J Clin Invest* 2017, **127:**3240-3249.

5. Lambert JC, Ibrahim-Verbaas CA, Harold D, Naj AC, Sims R, Bellenguez C, DeStafano AL, Bis JC, Beecham GW, Grenier-Boley B, et al: **Meta-analysis of 74,046 individuals identifies 11 new susceptibility loci for Alzheimer's disease.** *Nat Genet* 2013, **45:**1452-1458.

6. Efthymiou AG, Goate AM: **Late onset Alzheimer's disease genetics implicates microglial pathways in disease risk.** *Molecular Neurodegeneration* 2017, **12:**43.

7. Durafourt BA, Moore CS, Zammit DA, Johnson TA, Zaguia F, Guiot MC, Bar-Or A, Antel JP: **Comparison of polarization properties of human adult microglia and blood-derived macrophages.** *Glia* 2012, **60:**717-727.

8. Bennett ML, Bennett FC, Liddelow SA, Ajami B, Zamanian JL, Fernhoff NB, Mulinyawe SB, Bohlen CJ, Adil A, Tucker A, et al: **New tools for studying microglia in the mouse and human CNS.** *Proc Natl Acad Sci U S A* 2016, **113:**E1738-1746.

9. Zhang Y, Chen K, Sloan SA, Bennett ML, Scholze AR, O'Keeffe S, Phatnani HP, Guarnieri P, Caneda C, Ruderisch N, et al: **An RNA-sequencing transcriptome and splicing database of glia, neurons, and vascular cells of the cerebral cortex.** *J Neurosci* 2014, **34:**11929-11947.

10. Gosselin D, Skola D, Coufal NG, Holtman IR, Schlachetzki JCM, Sajti E, Jaeger BN, O'Connor C, Fitzpatrick C, Pasillas MP, et al: **An environment-dependent transcriptional network specifies human microglia identity.** *Science* 2017, **356**.

11. Keren-Shaul H, Spinrad A, Weiner A, Matcovitch-Natan O, Dvir-Szternfeld R, Ulland TK, David E, Baruch K, Lara-Astaiso D, Toth B, et al: **A Unique Microglia Type Associated with Restricting Development of Alzheimer's Disease.** *Cell* 2017, **169:**1276-1290 e1217.

12. Friedman BA, Srinivasan K, Ayalon G, Meilandt WJ, Lin H, Huntley MA, Cao Y, Lee SH, Haddick PCG, Ngu H, et al: **Diverse Brain Myeloid Expression Profiles Reveal Distinct Microglial Activation States and Aspects of Alzheimer's Disease Not Evident in Mouse Models.** *Cell Rep* 2018, **22:**832-847.

13. Mathys H, Adaikkan C, Gao F, Young JZ, Manet E, Hemberg M, De Jager PL, Ransohoff RM, Regev A, Tsai LH: **Temporal Tracking of Microglia Activation in Neurodegeneration at Single-Cell Resolution.** *Cell Rep* 2017, **21:**366-380.

14. Chiu IM, Morimoto ET, Goodarzi H, Liao JT, O'Keeffe S, Phatnani HP, Muratet M, Carroll MC, Levy S, Tavazoie S, et al: **A neurodegeneration-specific gene-expression signature of acutely isolated microglia from an amyotrophic lateral sclerosis mouse model.** *Cell Rep* 2013, **4:**385-401.

15. Hammond TR, Dufort C, Dissing-Olesen L, Giera S, Young A, Wysoker A, Walker AJ, Gergits F, Segel M, Nemesh J, et al: **Single-Cell RNA Sequencing of Microglia throughout the Mouse Lifespan and in the Injured Brain Reveals Complex Cell-State Changes.** *Immunity* 2019, **50:**253-271 e256.

16. Rangaraju S, Dammer EB, Raza SA, Rathakrishnan P, Xiao H, Gao T, Duong DM, Pennington MW, Lah JJ, Seyfried NT, Levey AI: **Identification and therapeutic modulation of a pro-inflammatory subset of disease-associated-microglia in Alzheimer's disease.** *Mol Neurodegener* 2018, **13:**24.

17. de Sousa Abreu R, Penalva LO, Marcotte EM, Vogel C: **Global signatures of protein and mRNA expression levels.** *Mol Biosyst* 2009, **5:**1512-1526.

18. Vogel C, Marcotte EM: **Insights into the regulation of protein abundance from proteomic and transcriptomic analyses.** *Nat Rev Genet* 2012, **13:**227-232.

19. Maier T, Guell M, Serrano L: **Correlation of mRNA and protein in complex biological samples.** *FEBS Lett* 2009, **583:**3966-3973.

20. Sharma K, Schmitt S, Bergner CG, Tyanova S, Kannaiyan N, Manrique-Hoyos N, Kongi K, Cantuti L, Hanisch UK, Philips MA, et al: **Cell type- and brain region-resolved mouse brain proteome.** *Nat Neurosci* 2015, **18:**1819-1831.

21. Flowers A, Bell-Temin H, Jalloh A, Stevens SM, Jr., Bickford PC: **Proteomic anaysis of aged microglia: shifts in transcription, bioenergetics, and nutrient response.** *J Neuroinflammation* 2017, **14:**96.

22. Guergues J, Zhang P, Liu B, Stevens SM, Jr.: **Improved Methodology for Sensitive and Rapid Quantitative Proteomic Analysis of Adult-Derived Mouse Microglia: Application to a Novel In Vitro Mouse Microglial Cell Model.** *Proteomics* 2019, **19:**e1800469.

23. Rangaraju S, Dammer EB, Raza SA, Gao T, Xiao H, Betarbet R, Duong DM, Webster JA, Hales CM, Lah JJ, et al: **Quantitative proteomics of acutely-isolated mouse microglia identifies novel immune Alzheimer's disease-related proteins.** *Mol Neurodegener* 2018, **13:**34.

24. Bretscher A, Edwards K, Fehon RG: **ERM proteins and merlin: integrators at the cell cortex.** *Nat Rev Mol Cell Biol* 2002, **3:**586-599.

25. Berryman M, Franck Z, Bretscher A: **Ezrin is concentrated in the apical microvilli of a wide variety of epithelial cells whereas moesin is found primarily in endothelial cells.** *J Cell Sci* 1993, **105 (Pt 4):**1025-1043.

26. Shcherbina A, Bretscher A, Kenney DM, Remold-O'Donnell E: **Moesin, the major ERM protein of lymphocytes and platelets, differs from ezrin in its insensitivity to calpain.** *FEBS Lett* 1999, **443:**31-36.

27. Faure S, Salazar-Fontana LI, Semichon M, Tybulewicz VL, Bismuth G, Trautmann A, Germain RN, Delon J: **ERM proteins regulate cytoskeleton relaxation promoting T cell-APC conjugation.** *Nat Immunol* 2004, **5:**272-279.

28. Littman DR: **An inducible cre recombinase driven by Cx3cr1.** *MGI Direct Data Submission* 2013.

29. Liao C, Prabhu KS, Paulson RF: **Monocyte-derived macrophages expand the murine stress erythropoietic niche during the recovery from anemia.** *Blood* 2018, **132:**2580-2593.

30. Esser J, Rakonjac M, Hofmann B, Fischer L, Provost P, Schneider G, Steinhilber D, Samuelsson B, Radmark O: **Coactosin-like protein functions as a stabilizing chaperone for 5-lipoxygenase: role of tryptophan 102.** *Biochem J* 2009, **425:**265-274.

31. Kim J, Shapiro MJ, Bamidele AO, Gurel P, Thapa P, Higgs HN, Hedin KE, Shapiro VS, Billadeau DD: **Coactosin-like 1 antagonizes cofilin to promote lamellipodial protrusion at the immune synapse.** *PLoS One* 2014, **9:**e85090.

32. Seyfried NT, Dammer EB, Swarup V, Nandakumar D, Duong DM, Yin L, Deng Q, Nguyen T, Hales CM, Wingo T, et al: **A Multi-network Approach Identifies Protein-Specific Co-expression in Asymptomatic and Symptomatic Alzheimer's Disease.** *Cell Syst* 2017, **4:**60-72 e64.

33. Umoh ME, Dammer EB, Dai J, Duong DM, Lah JJ, Levey AI, Gearing M, Glass JD, Seyfried NT: **A proteomic network approach across the ALS-FTD disease spectrum resolves clinical phenotypes and genetic vulnerability in human brain.** *EMBO Mol Med* 2018, **10:**48-62.

34. Chen WT, Lu A, Craessaerts K, Pavie B, Frigerio CS, Mancuso R, Qian X, Lalakova J, Kühnemund M, Voytyuk I, et al: **Spatial and temporal transcriptomics reveal microglia-astroglia crosstalk in the amyloid-β plaque cell niche of Alzheimer's disease.** *bioRxiv* 2019.

35. Zhang B, Gaiteri C, Bodea LG, Wang Z, McElwee J, Podtelezhnikov AA, Zhang C, Xie T, Tran L, Dobrin R, et al: **Integrated systems approach identifies genetic nodes and networks in late-onset Alzheimer's disease.** *Cell* 2013, **153:**707-720.

36. Masuda T, Sankowski R, Staszewski O, Bottcher C, Amann L, Sagar, Scheiwe C, Nessler S, Kunz P, van Loo G, et al: **Spatial and temporal heterogeneity of mouse and human microglia at single-cell resolution.** *Nature* 2019, **566:**388-392.

37. Bottcher C, Schlickeiser S, Sneeboer MAM, Kunkel D, Knop A, Paza E, Fidzinski P, Kraus L, Snijders GJL, Kahn RS, et al: **Human microglia regional heterogeneity and**

phenotypes determined by multiplexed single-cell mass cytometry. *Nat Neurosci* 2019, **22:**78-90.

38. Ting L, Rad R, Gygi SP, Haas W: **MS3 eliminates ratio distortion in isobaric multiplexed quantitative proteomics.** *Nat Methods* 2011, **8:**937-940.

39. McAlister GC, Nusinow DP, Jedrychowski MP, Wuhr M, Huttlin EL, Erickson BK, Rad R, Haas W, Gygi SP: **MultiNotch MS3 enables accurate, sensitive, and multiplexed detection of differential expression across cancer cell line proteomes.** *Anal Chem* 2014, **86:**7150-7158.

40. Ping L, Duong DM, Yin L, Gearing M, Lah JJ, Levey AI, Seyfried NT: **Global quantitative analysis of the human brain proteome in Alzheimer's and Parkinson's Disease.** *Sci Data* 2018, **5:**180036.

41. Thompson A, Schafer J, Kuhn K, Kienle S, Schwarz J, Schmidt G, Neumann T, Johnstone R, Mohammed AK, Hamon C: **Tandem mass tags: a novel quantification strategy for comparative analysis of complex protein mixtures by MS/MS.** *Anal Chem* 2003, **75:**1895-1904.

42. Swartzlander DB, Propson NE, Roy ER, Saito T, Saido T, Wang B, Zheng H: **Concurrent cell type-specific isolation and profiling of mouse brains in inflammation and Alzheimer's disease.** *JCI Insight* 2018, **3**.

43. Lankes WT, Furthmayr H: **Moesin: a member of the protein 4.1-talin-ezrin family of proteins.** *Proc Natl Acad Sci U S A* 1991, **88:**8297-8301.

44. Kall L, Canterbury JD, Weston J, Noble WS, MacCoss MJ: **Semi-supervised learning for peptide identification from shotgun proteomics datasets.** *Nat Methods* 2007, **4:**923-925.

45. Dai J, Johnson ECB, Dammer EB, Duong DM, Gearing M, Lah JJ, Levey AI, Wingo TS, Seyfried NT: **Effects of APOE Genotype on Brain Proteomic Network and Cell Type Changes in Alzheimer's Disease.** *Front Mol Neurosci* 2018, **11:**454.

46. Schindelin J, Arganda-Carreras I, Frise E, Kaynig V, Longair M, Pietzsch T, Preibisch S, Rueden C, Saalfeld S, Schmid B, et al: **Fiji: an open-source platform for biological-image analysis.** *Nat Methods* 2012, **9:**676-682.

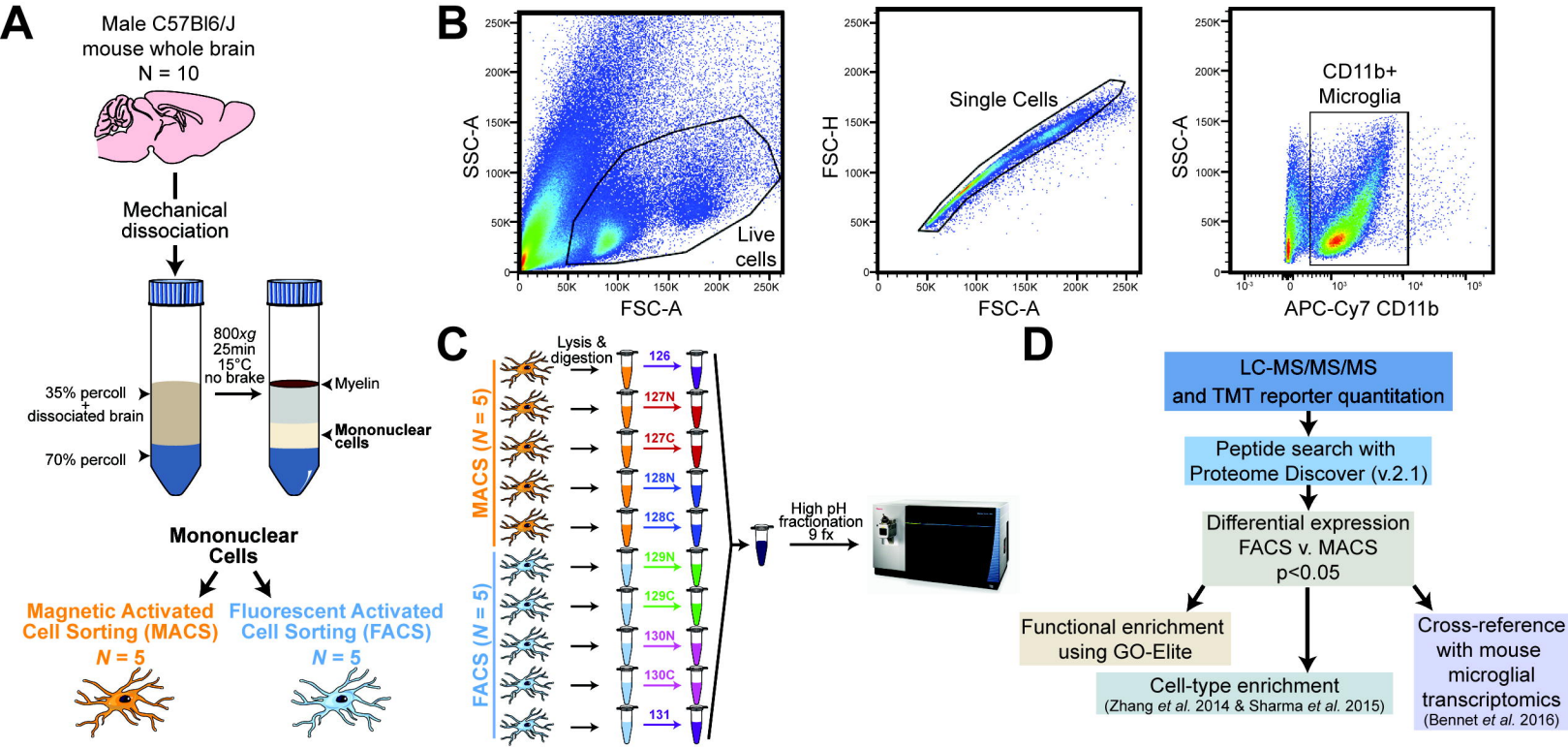
A
Male C57Bl6/J
mouse whole brain
N = 10
Mechanical
dissociation
800xg
25min
15°C
no brake
35% percoll
+
dissociated brain
70% percoll
Myelin
Mononuclear
cells
Mononuclear
Cells
Magnetic Activated
Cell Sorting (MACS)
N = 5
Fluorescent Activated
Cell Sorting (FACS)
N = 5
B
SSC-A
FSC-A
Live
cells
FSC-H
Single Cells
CD11b+
Microglia
APC-Cy7 CD11b
C
Lysis &
digestion
MACS (N = 5)
FACS (N = 5)
126
127N
127C
128N
128C
129N
129C
130N
130C
131
High pH
fractionation
9 fx
D
LC-MS/MS/MS
and TMT reporter quantitation
Peptide search with
Proteome Discover (v.2.1)
Differential expression
FACS v. MACS
p<0.05
Functional enrichment
using GO-Elite
Cell-type enrichment
(Zhang et al. 2014 & Sharma et al. 2015)
Cross-reference
with mouse
microglial
transcriptomics
(Bennet et al. 2016)

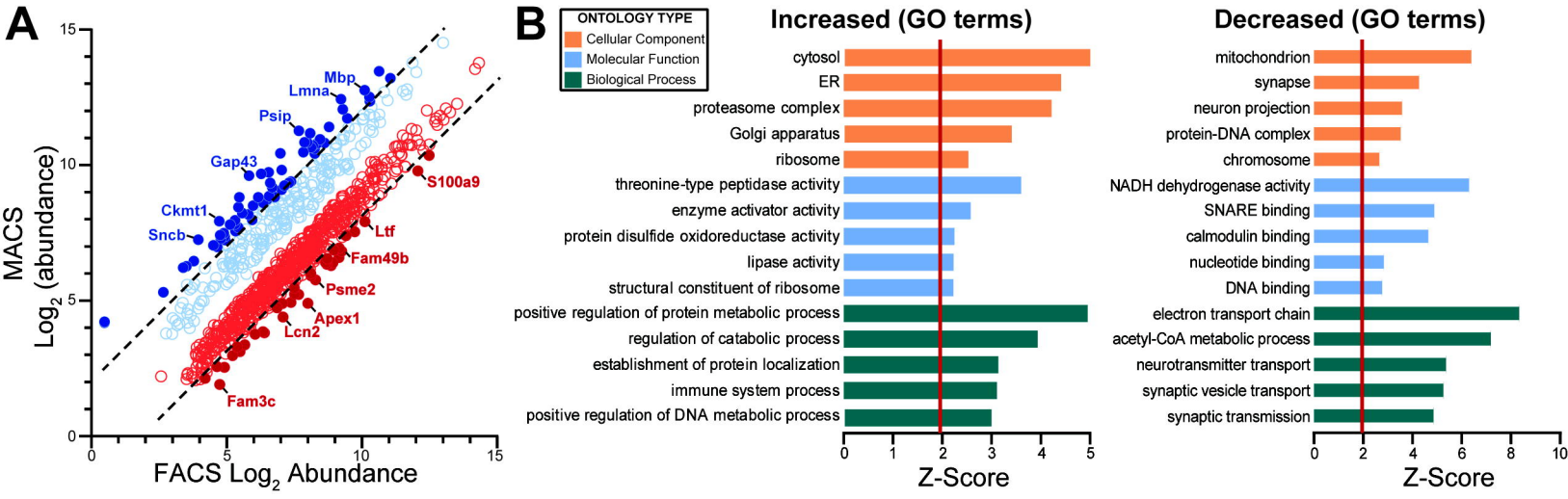
A
MACS
Log2 (abundance)
FACS Log2 Abundance
Mbp
Lmna
Psip
Gap43
Ckmt1
Sncb
S100a9
Ltf
Fam49b
Psme2
Apex1
Lcn2
Fam3c
B
ONTOLOGY TYPE
Cellular Component
Molecular Function
Biological Process
Increased (GO terms)
cytosol
ER
proteasome complex
Golgi apparatus
ribosome
threonine-type peptidase activity
enzyme activator activity
protein disulfide oxidoreductase activity
lipase activity
structural constituent of ribosome
positive regulation of protein metabolic process
regulation of catabolic process
establishment of protein localization
immune system process
positive regulation of DNA metabolic process
Z-Score
Decreased (GO terms)
mitochondrion
synapse
neuron projection
protein-DNA complex
chromosome
NADH dehydrogenase activity
SNARE binding
calmodulin binding
nucleotide binding
DNA binding
electron transport chain
acetyl-CoA metabolic process
neurotransmitter transport
synaptic vesicle transport
synaptic transmission
Z-Score

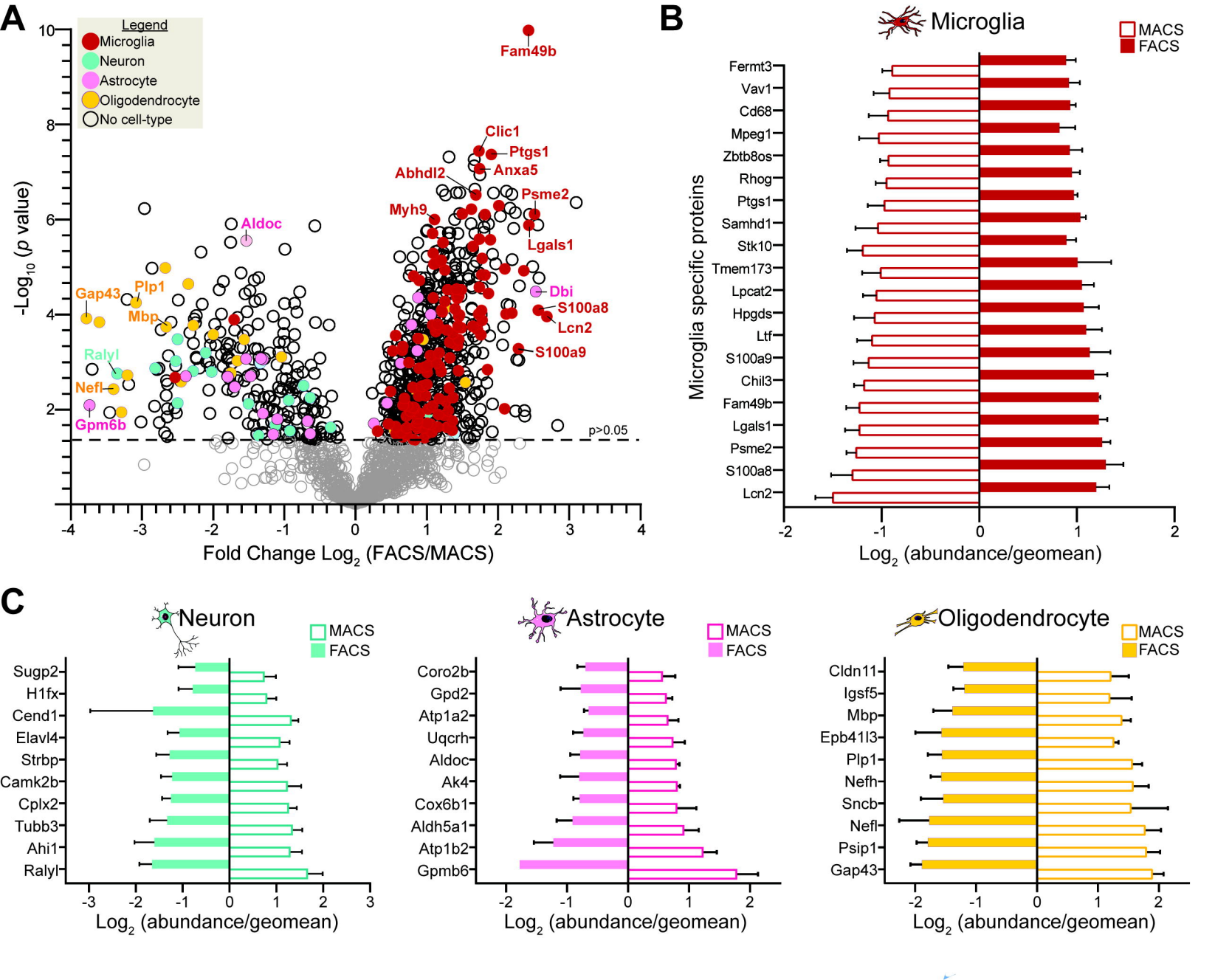
A
Legend
Microglia
Neuron
Astrocyte
Oligodendrocyte
No cell-type
Fam49b
Clic1
Ptgs1
Anxa5
Abhdl2
Psme2
Myh9
Aldoc
Lgals1
Dbi
S100a8
Lcn2
S100a9
Gap43
Plp1
Mbp
Ralyl
Nefl
Gpm6b
p>0.05
-Log10 (p value)
Fold Change Log2 (FACS/MACS)
B
Microglia
MACS
FACS
Microglia specific proteins
Fermt3
Vav1
Cd68
Mpeg1
Zbtb8os
Rhog
Ptgs1
Samhd1
Stk10
Tmem173
Lpcat2
Hpgds
Ltf
S100a9
Chil3
Fam49b
Lgals1
Psme2
S100a8
Lcn2
Log2 (abundance/geomean)
C
Neuron
MACS
FACS
Sugp2
H1fx
Cend1
Elavl4
Strbp
Camk2b
Cplx2
Tubb3
Ahi1
Ralyl
Log2 (abundance/geomean)
Astrocyte
MACS
FACS
Coro2b
Gpd2
Atp1a2
Uqcrh
Aldoc
Ak4
Cox6b1
Aldh5a1
Atp1b2
Gpmb6
Log2 (abundance/geomean)
Oligodendrocyte
MACS
FACS
Cldn11
Igsf5
Mbp
Epb41l3
Plp1
Nefh
Sncb
Nefl
Psip1
Gap43
Log2 (abundance/geomean)

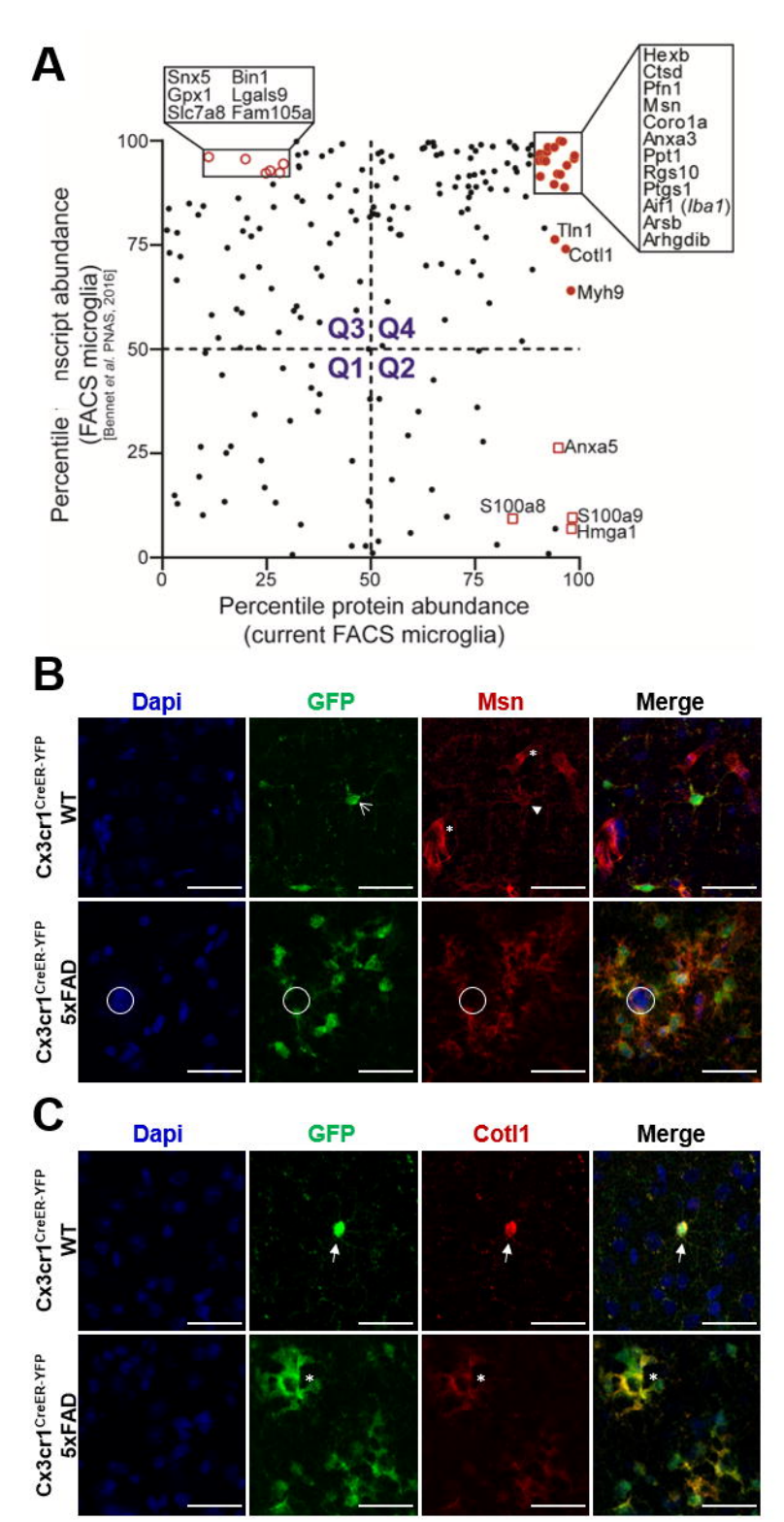
A
Snx5 Bin1
Gpx1 Lgals9
Slc7a8 Fam105a
Hexb
Ctsd
Pfn1
Msn
Coro1a
Anxa3
Ppt1
Rgs10
Ptgs1
Aif1 (Iba1)
Arsb
Arhgdib
Tln1
Cotl1
Myh9
Q3 Q4
Q1 Q2
Anxa5
S100a8
S100a9
Hmga1
Percentile transcript abundance
(FACS microglia)
[Bennet et al. PNAS, 2016]
Percentile protein abundance
(current FACS microglia)
0
25
50
75
100
B
Dapi
GFP
Msn
Merge
Cx3cr1CreER-YFP WT
Cx3cr1CreER-YFP 5xFAD
C
Dapi
GFP
Cotl1
Merge
Cx3cr1CreER-YFP WT
Cx3cr1CreER-YFP 5xFAD